

Fundamentals of Time-Resolved Charge-Transfer in Time-Dependent Density Functional Theory

J. I. Fuks,¹ P. Elliott,² A. Rubio,^{1,3} and N. T. Maitra²

¹Nano-Bio Spectroscopy group, Dpto. Física de Materiales, Universidad del País Vasco, Centro de Física de Materiales CSIC-UPV/EHU-MPC and DIPC, Av. Tolosa 72, E-20018 San Sebastián, Spain

²Department of Physics and Astronomy, Hunter College and the City

University of New York, 695 Park Avenue, New York, New York 10065, USA

³Fritz-Haber-Institut der Max-Planck-Gesellschaft, Faradayweg 4-6, D-14195 Berlin, Germany

(Dated: November 14, 2012)

We show that as an electron transfers between closed-shell molecular fragments at large separation, the exact correlation potential of time-dependent density functional theory gradually develops a step and peak structure in the bonding region. This structure has a density-dependence that is non-local both in space and time, and even the exact ground-state exchange-correlation functional fails to capture it. In the complementary case of charge-transfer between open-shell fragments, an initial step and peak vanish as the charge-transfer state is reached. Lack of these structures in usual approximations leads to inaccurate charge-transfer dynamics. This is dramatically illustrated by the complete lack of Rabi oscillations in the dipole moment under conditions of resonant charge-transfer.

Charge-transfer dynamics play a critical role in many processes of interest in physics, chemistry, and biochemistry, from photochemistry to photosynthesis, solar cell design and biological functionality. The quantum mechanical treatment of such systems calls for methods that can treat correlated electron excitations and dynamics efficiently for relatively large systems. Time-dependent density functional theory (TDDFT) [1, 2] is the leading candidate today, and has achieved an unprecedented balance between accuracy and efficiency in calculations of electronic spectra [2, 3]. Charge-transfer excitation energies over medium to large distances are, however, notoriously underestimated by the usual exchange-correlation (xc) functionals, and recent years have witnessed intense development of many methods to treat it [4–6]. There is recent optimism for obtaining accurate charge-transfer excitations [5] but only for the case of charge-transfer between closed-shell fragments. No functional approximation developed so far works for charge-transfer between open-shell fragments [7, 8]. Here standard approximations predict even an unphysical ground-state with fractionally-charged species in the dissociation limit. For open-shell fragments the exact ground-state correlation potential has step and peak structures [9, 10], while the exact exchange-correlation kernel has strong frequency-dependence and diverges as a function of the fragment separation; lack of these features in the usual (TD)DFT approximations is responsible for their poor predictions.

In contrast to linear response phenomena, the description of important photophysical/chemical processes such as excited state reactivity, photoisomerisation, photofragmentation, electron and proton transfer and electron-hole recombination, generally requires a complete electron transfer from one state to another, or from different regions of space. All those processes are clearly nonlinear and require a non-perturbative *time-resolved* study of electron dynamics rather than a cal-

ulation of the excitation spectrum of the unperturbed system. TDDFT still applies: non-interacting electrons evolve in a one-body time-dependent Kohn-Sham (KS) potential, in principle reproducing the exact one-body density of the true interacting system and from which all properties of the interacting system may be exactly extracted. In practise, approximations are required for the many-body effects, in particular the xc potential, $v_{xc}[n; \Psi_0, \Phi_0](\mathbf{r}, t)$, a functional of the one-body density n , the initial interacting state Ψ_0 and the initial KS state Φ_0 . Almost all calculations today use an adiabatic approximation, that inserts the instantaneous density into a ground-state approximation, $v_{xc}^{adia}[n; \Psi_0, \Phi_0](\mathbf{r}, t) = v_{xc}^{g.s.}[n(t)](\mathbf{r}, t)$, neglecting the dependence of v_{xc} on the past history and initial states [2]. Further, while the exact v_{xc} has in general a non-local dependence on space, the ground-state approximation most often has a spatially local or semi-local dependence on the density [23].

How would these approximations perform for the time-resolved charge-transfer process? In this paper, we unambiguously show that when an electron transfers at long range from a ground-state to an excited charge-transfer state, a time-dependent step and peak are generic and essential features of the xc potential. In the case where the donor and acceptor are both closed shells, the initial potential has no step nor peak, but a step and peak structure in the bond midpoint region of the xc potential builds up over time. Although initially the usual approximations may be good approximations to the exact xc potential, they are increasingly worse as time evolves, leading to a completely wrong long-time dynamics. The reverse is true in the case where the donor and acceptor are both open-shell species. Thus the step and peak, spatially non-local features that are difficult to capture in functional approximations, play a significant role *even in charge-transfer between closed-shell fragments, unlike in the calculation of excitation energies*. Further, we show that although an adiabatic ap-

proximation to the xc potential may yield a step structure, the step will, at best, be of the wrong size. Accompanying the step and peak structures associated with the charge transfer there is also typically a generic dynamical step [12], that depends on details of how the charge-transfer is achieved. The structure of the exact v_{xc} functional thus has a complicated space- and time-dependence that adiabatic functionals fail to capture. The consequence for the time-resolved dynamics is severe, as we will show under conditions of resonant charge-transfer.

To illustrate the mechanism of charge-transfer processes and the relevance of spatial and time non-locality we use a “two-electron molecule” in one-dimension. The Hamiltonian is (atomic units are used throughout):

$$H(x_1, x_2, t) = -\frac{1}{2} \frac{\partial^2}{\partial x_1^2} - \frac{1}{2} \frac{\partial^2}{\partial x_2^2} + v_{\text{mol}}(x_1) + v_{\text{mol}}(x_2) + v_{\text{ee}}(x_1 - x_2) + \mathcal{E}(t) \cdot (x_1 + x_2) \quad (1)$$

where $v_{\text{ee}}(y) = 1/\sqrt{y^2 + 1}$ is the “soft-Coulomb” electron-electron interaction, and $\mathcal{E}(t) = A \cos(\omega t)$ is an applied electric field. The neutral molecule is modeled by:

$$v_{\text{mol}}(x) = -\frac{Z}{\sqrt{(x + \frac{R}{2})^2 + a}} - \frac{U_0}{\cosh^2(x - \frac{R}{2})} \quad (2)$$

Asymptotically the soft-coulomb potential (donor) on the left decays as $-Z/x$, similar to a true atomic potential in 3D, while the cosh-squared (acceptor) on the right is short-ranged, decaying exponentially away from the “atom”. The acceptor potential mimics a closed-shell atom without including core electrons. By varying the parameters Z and U_0 , the character of the ground and excited states change. We model charge-transfer between two closed-shell fragments, by choosing Z and U_0 such that, at large separations R , the ground-state has two electrons on the donor and zero on the acceptor, while the first singlet excited state, Ψ^* , is a charge-transfer excited state with one electron in each well (see Fig. 1). The applied electric field $\mathcal{E}(t)$ induces this charge transfer. For this case we choose $Z = 2$ and $U_0 = 1$. Choosing $Z = 2$ and $U_0 = 1.5$ places one electron in each well in the ground-state, with a charge-transfer excited state having both electrons in the acceptor well; such a system would be used in modeling charge-transfer between two open-shell fragments.

If we consider beginning the KS simulation in a doubly-occupied singlet state, KS evolution retains this form for all later times, $\Phi(x_1, x_2, t) = \phi(x_1, t)\phi(x_2, t)$, and requiring the exact density to be reproduced at all times leads to the expression:

$$\phi(x, t) = \sqrt{n(x, t)/2} e^{i \int^x dx' u(x', t)} \quad (3)$$

where $u(x, t) = j(x, t)/n(x, t)$ is the local “velocity”. In-

verting the KS equation yields the KS potential as:

$$v_{\text{S}}(x, t) = \frac{\partial_x^2 n(x, t)}{4n(x, t)} - \frac{(\partial_x n(x, t))^2}{8n^2(x, t)} - \frac{u^2(x, t)}{2} - \int^x \partial_t u(x', t) dx' \quad (4)$$

The xc potential is then found via

$$v_{\text{xc}}(x, t) = v_{\text{S}}(x, t) - v_{\text{ext}}(x, t) - v_{\text{H}}(x, t) \quad (5)$$

where $v_{\text{H}}(x, t) = \int dx' n(x', t) v_{\text{ee}}(x - x')$ is the Hartree potential and the external field is given by $v_{\text{ext}}(x, t) = v_{\text{mol}}(x) + \mathcal{E}(t)x$. Further, for this case, $v_{\text{C}}(x, t) = v_{\text{xc}} - v_{\text{x}}(x, t)$, may easily be isolated since $v_{\text{x}} = -v_{\text{H}}/2$.

Before discussing the time-dependent electron dynamics, we first consider the final charge-transfer state. Let us assume we have complete transfer of an electron at some time T into the excited state Ψ^* (for example using a tailored laser pulse, which is then turned off), and the system then stays in this state for all times $t > T$. The density, $n(t > T) = n^*$, is then static in the excited state, and the current and velocity $u(x, t)$ are zero. It follows that the exact $v_{\text{xc}}(t > T)$ is static and that the exact KS potential is given by first two terms of Eq. (4) only.

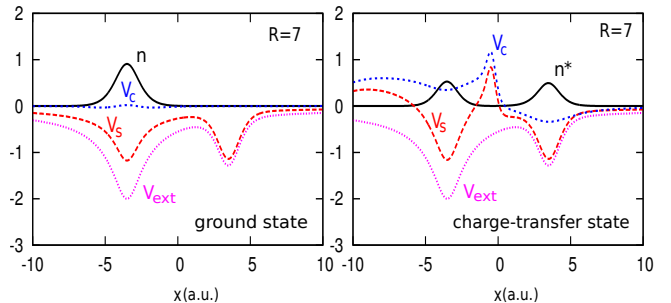


FIG. 1: Density (black solid), v_{S} (red long-dashed), v_{C} (blue dashed), and v_{ext} (pink dotted) for the ground-state (left) and for the charge-transfer state (right) in our model molecule of closed-shell fragments at separation $R = 7\text{au}$.

In Fig. 1, we show the density and the exact KS and correlation potentials for the ground and charge-transfer states for separation $R = 7\text{au}$. A clear step and peak structure has developed in the correlation potential in the region of low-density between the ions in the charge-transfer state. There is no such structure in the initial potential of the ground-state. As the separation increases, the step in v_{C} saturates to a size

$$\Delta = |I_D^{N_D-1} - I_A^{N_A+1}|, \quad (6)$$

where $I_D^{N_D-1} = I_D^{N=1}$ is the ionization energy of the donor ion containing one electron, $I_A^{N_A+1} = I_A^{N=1}$ is that of the one-electron acceptor ion, and $N_D(N_A)$ represent the number of electrons of the donor(acceptor) ion. This can readily be shown by considering the asymptotic decay of the donor and acceptor KS orbitals, following similar arguments to Refs. [9, 10] that hold for

the case of the *ground-state* of a molecule made of *open-shell* fragments. Here instead, we have a step in the the correlation potential of a charge-transfer excited-state of a molecule made of closed-shell fragments.

The step requires a spatially non-local density-dependence in the correlation functional, as described for the ground-state case in Refs.[9, 10, 13, 14]. The inability of usual ground-state approximate functionals to capture this step results in them incorrectly predicting fractionally charged species. Here we are studying an excited state of the interacting system. However the KS orbital is in fact a ground-state orbital, because the excited-state one-body density has no nodes. Given the static ground-state nature of the orbital and KS potentials after time T , does the adiabatic approximation become exact?

To answer this, we examine the *adiabatically exact* xc potential for $t > T$, $v_{\text{xc}}^{\text{adia-ex}}[n^*]$, i.e. evaluating the exact ground-state xc functional on the instantaneous charge-transfer density. This is defined as [17]:

$$v_{\text{xc}}^{\text{adia-ex}}[n] = v_{\text{s}}^{\text{adia}}[n] - v_{\text{ext}}^{\text{adia}}[n] - v_{\text{H}}[n] \quad (7)$$

where $v_{\text{ext}}^{\text{adia}}[n]$ is the external potential for two interacting electrons in a ground-state of this density, and $v_{\text{s}}^{\text{adia}}[n]$ is the exact ground-state KS potential for this density (first two terms of Eq. (4)).

In Fig. 2 we plot the $v_{\text{xc}}^{\text{adia-ex}}[n^*]$ for two separations $R = 7\text{au}$ and 10au , found using similar numerical techniques to Refs. 17 and 18. Evidently, the adiabatic approximation does yield a step, but of the wrong size.

To understand this, first consider the functional dependence of the exact xc potential. We may write

$$v_{\text{xc}}[n](t > T) = v_{\text{xc}}[n^*, \Psi^*, \Phi_{CT}^{\text{gs}}](t > T), \quad (8)$$

where, on the left, the dependence is on the entire history of the density, $n(0 < t < T)$, and initial-state dependence is not needed since at the initial time the interacting and KS states are at the ground-state [2, 19]. On the right, history-dependence has been “traded” for initial-state dependence; time T is considered as the “initial” time, and the functional depends on just the static density n^* after this time, and, crucially, the interacting state and KS states at time T . The former is the charge-transfer excited state Ψ^* , while the latter is the doubly-occupied orbital, $\Phi(x_1, x_2, T) = \sqrt{n^*(x_1)n^*(x_2)}/2 \equiv \Phi_{CT}^{\text{gs}}$, a ground-state wavefunction, as discussed above.

On the other hand, the adiabatic approximation for the xc potential

$$v_{\text{xc}}^{\text{adia}}[n^*] \equiv v_{\text{xc}}^{\text{adia}}[n^*, \Psi_{CT}^{\text{gs}}, \Phi_{CT}^{\text{gs}}], \quad (9)$$

differs from the exact xc potential Eq. (8), in its dependence on the time- T interacting state: here Ψ_{CT}^{gs} is the *ground-state* wavefunction of an interacting system with density n^* , *not the true excited state wavefunction*. Therefore, Eqs. (8) and (9) show that the adiabatically-exact xc potential is not the same as the exact xc potential. In the

infinite-separation limit, we expect Ψ^* and Ψ_{CT}^{gs} to be very similar, both having a Heitler-London form with one electron in each well, but the fact that Ψ^* is an excited state is encoded in the nodal structure of its wavefunction. The correlation potential is extremely sensitive to this tiny difference in the two interacting wavefunctions, which accounts for the different step size in Fig. 2.

The magnitude of the step in $v_{\text{xc}}^{\text{adia-ex}}$ in the infinite-separation limit can be derived by examining the terms in Eq. (7). In this limit, locally around each well $v_{\text{ext}}^{\text{adia}}$ must be the atomic potential, up to a spatial constant, in order for $\Psi_{CT}^{\text{gs}}[n^*]$ to satisfy Schrödinger’s equation there. It cannot simply be the sum of the atomic potentials, because the ground-state Ψ_0 of that potential (Eq. 2) places two electrons in the donor well. For Ψ_{CT}^{gs} to be the ground-state wavefunction, $v_{\text{ext}}^{\text{adia}}$ has a step in the region of negligible density that pushes up the donor well relative to the acceptor well; the size of this step, C , is the lowest such that energetically it is favorable to place one electron on each well, as $\Psi_{CT}^{\text{gs}}[n^*]$ does. So,

$$E_D^{\text{gs}, N=1} + E_A^{\text{gs}, N=1} + C < E_D^{\text{gs}, N=2} + 2C \quad (10)$$

where the left-hand-side represents the energy $E[\Psi_{CT}^{\text{gs}}]$ and the right-hand-side represents the energy of the lowest state of $v_{\text{ext}}^{\text{adia}}$ that has two electrons in the donor well. This leads to

$$C \geq E_D^{\text{gs}, N=1} + E_A^{\text{gs}, N=1} - E_D^{\text{gs}, N=2} \quad (11)$$

$$= A_D^{N=1} - I_A^{N=1} = I_D^{N=D} - I_A^{N=A} \quad (12)$$

where in the last line, we have generalized the result to a donor(acceptor) with $N_D(N_A)$ electrons.

Now that we have the magnitude of the step in $v_{\text{ext}}^{\text{adia}}[n^*]$, we use Eq. (7) to quantify the step in $v_{\text{xc}}^{\text{adia-ex}}[n^*]$. Since $v_{\text{s}}^{\text{adia}} = v_{\text{s}}^{\text{exact}}$ here, Eq. 6 tells us that the step in $v_{\text{c}}^{\text{adia}}$ is

$$\Delta_{\text{adia}} = I_D^{N_D-1} - A_D^{N_D-1} \quad (13)$$

which is equal to the *derivative discontinuity* of the $(N_D - 1)$ -electron donor. (As before, we note that the entire step is contained in the correlation part of the potential, because with the doubly-occupied orbital, $v_{\text{x}} = -v_{\text{H}}/2$). For our system $I_D^{N=1} = 1.483\text{au}$, $A_D^{N=1} = 0.755\text{au}$ and $I_A^{N=1} = 0.5\text{au}$, thus in the infinite separation limit we get a step of $0.983(0.729)\text{au}$ in the exact $v_{\text{c}}(v_{\text{c}}^{\text{adia}})$. The numerical results verify this analysis; the steps shown in Figure 2 for separation $R = 7(R = 10)\text{au}$ have values of $0.61(0.76)\text{au}$ in the exact v_{c} and $0.42(0.55)\text{au}$ in $v_{\text{c}}^{\text{adia}}$. For larger separations, the steps tend towards the asymptotic values predicted by the analysis above.

Having studied how the xc potential looks for the final charge-transfer state, we now study how the potential evolves in time to reach such a state. To greatly simplify the analysis we will exploit Rabi physics to reduce this to a two-state problem. This approach is justified for weak-enough resonant driving, and verified by comparing the xc potential found via this approach with that found using the exact time-dependent

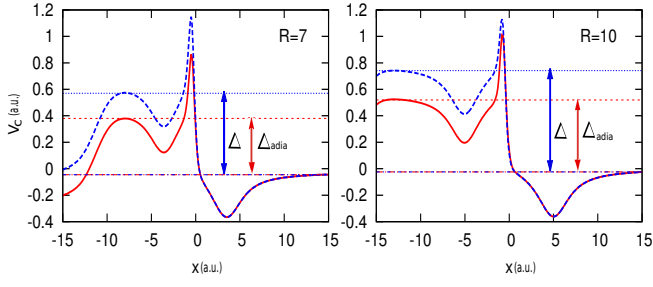


FIG. 2: The exact v_C (dashed blue line) and the adiabatic exact v_C^{adia} (red solid line) for $R = 7$ au (left) and for $R = 10$ au (right). Note that the potential eventually rolls back down to zero far enough away from the system. In the infinite separation limit the size of the step Δ (Δ_{adia}) is given by Eq. (6) (Eq. (13)).

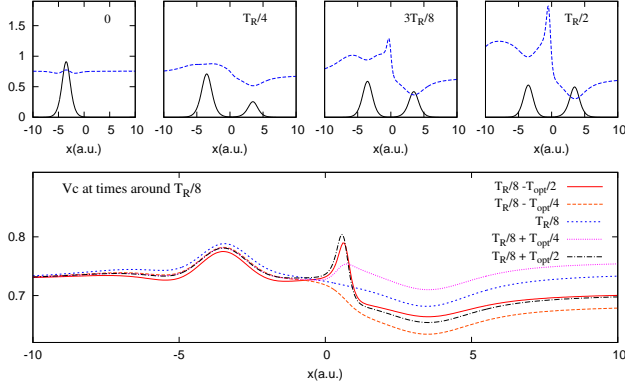


FIG. 3: Upper panel: The correlation potential (dotted blue line) and density (solid black) shown at snapshots of time indicated. Lower panel: V_c at snapshots over an optical cycle centered around $T_R/8$.

wavefunction found using octopus [15, 16] (see also Ref.12). The interacting wavefunction may be written as $|\Psi(t)\rangle = a_g(t)|\Psi^{gs}\rangle + a_e(t)|\Psi^*\rangle$, where

$$i\partial_t \begin{pmatrix} a_g(t) \\ a_e(t) \end{pmatrix} = \begin{pmatrix} E_g - d_{gg}\mathcal{E}(t) & -d_{eg}\mathcal{E}(t) \\ -d_{eg}\mathcal{E}(t) & E_e - d_{ee}\mathcal{E}(t) \end{pmatrix} \begin{pmatrix} a_g(t) \\ a_e(t) \end{pmatrix} \quad (14)$$

with $d_{eg} = d_{ge} = 0.231$, $d_{gg} = 7$ and $d_{ee} = 0$ for our system. The strength of the field is chosen to be $A = 0.006$. The electric field is resonant with the first excitation: $\mathcal{E}(t) = 0.006 \cos(0.112t)$.

Fig. 3 displays the correlation potential at snapshots in time over a half Rabi period $T_R/2$ [24] for separation $R = 7$. The step, accompanied by a peak, develops over time as the excited charge-transfer state is reached; at $T_R/2$ the correlation potential agrees with the static prediction earlier (see Fig. 2, left). Notice that making a time-dependent constant shift to the correlation potential does not affect the dynamics, just adds a time-

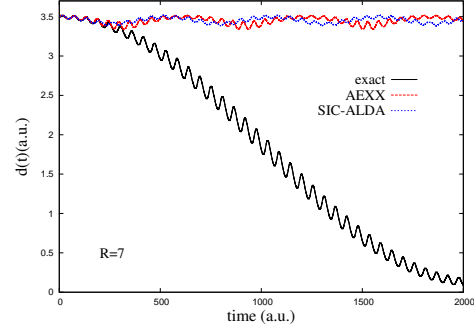


FIG. 4: Dipole moments $d(t)$ for the charge-transfer between closed-shell fragments at separation $R = 7$ au for exact (solid black line), adiabatic exact-exchange (AEEX) (dashed red line) and self-interaction-corrected adiabatic local density approximation (SIC-ALDA) (dotted blue line). The calculations were done using a resonant field of frequency $\omega = 0.112$ and amplitude $A = 0.00667$.

dependent overall phase. During the second half of the Rabi cycle, the step gradually disappears. A closer inspection however indicates that superimposed on this smoothly developing step, is an oscillatory step structure, whose dynamics is more on the time-scale of the optical field (see lower panel). This faster non-adiabatic, non-local dynamical step appears generically in electron dynamics, as shown in Ref. [12]. To distinguish between the two steps we refer to the more gradually developing step due to charge-transfer, as the “charge-transfer step”.

For charge-transfer between open-shells, somewhat of the reverse picture occurs: the initial correlation potential contains a step and peak [9, 10, 13, 14], that disappears in time as the charge-transfer state is reached. When studying this process using two electrons however, complications due to non- v -representability arise [20]; at large separations one approaches a node in the density in the excited-state, leading to a node in the single orbital that is doubly-occupied, giving delta-like peaks in the potential.

The impact that the development, or loss, of the charge-transfer step has on dynamics is severe. The same adiabatic approximations that for local resonant excitations showed faster but still Rabi-like oscillations [21] fail dramatically to capture *any* Rabi-like oscillations between the ground and charge-transfer state. This is illustrated by the dipole moments, $d(t) = \langle \psi(t) | \hat{x}_1 + \hat{x}_2 | \psi(t) \rangle$, in Figure (4). The approximate correlation functionals lack the non-local spatial-dependence necessary to develop the charge-transfer step [25].

Given the ubiquity of charge-transfer dynamics in topical applications of TDDFT, it is critical to develop approximations with spatially non-local and non-adiabatic dependence. None of the available functionals today captures the peak and step structure that develop in the exact correlation potential as the charge

transfers, and they lead to drastically incorrect dynamics, e.g. dipole oscillations between the ground and charge-transfer states induced by a weak resonant field are completely lacking. Even an exact adiabatic approximation will be incorrect: a step and peak feature are captured but of the wrong size. Superimposed on the development of the charge-transfer step potential, are the generic oscillatory dynamical step and peak features recently discussed in Ref [12]: the time-scale of this feature depends on the details of how the charge-transfer is induced, e.g. they oscillate on the time-scale of a resonant optical field. The performance of a self-consistent propagation in such a potential is left for a future investigation, as is the role of the peak that accompanies the step. The relation of these structures to the derivative discontinuities shown in the xc kernel for charge-transfer excitations [6] will also be investigated.

Although the results have been presented here for two electrons, we expect they can be generalized to electron transfer in real molecular systems, as many cases of charge transfer dominantly involve the valence level. In modeling real systems the vibronic coupling introduces

a mixture of excited states that are not, in principle, fully populated. Still our findings apply, since for an ensemble of states we would also get charge-transfer steps and dynamical steps that would account for the population of each excited state contributing to the wave packet. Note that the step responsible for the charge-transfer appears as soon as the state starts to be populated. Our work opens the path towards the development of non-adiabatic functionals able to capture dynamical electron transfer processes.

Acknowledgments We gratefully acknowledge financial support from the National Science Foundation CHE-1152784 (PE and NTM) and US Department of Energy DE-SC0008623 (NTM), and a grant of computer time from the CUNY High Performance Computing Center under NSF Grants CNS-0855217. The European Research Council (ERC-2010- AdG -267374), Spanish: FIS2011- 65702- C02-01 and PIB2010US- 00652), Grupos Consolidados (IT-319-07), and EC project CRONOS (280879-2) and CNS- 0958379, are gratefully acknowledged. JIF acknowledges support from an FPI fellowship (FIS2007-65702- C02-01).

-
- [1] E. Runge and E.K.U. Gross, Phys. Rev. Lett. **52**, 997 (1984).
 [2] *Fundamentals of Time-Dependent Density Functional Theory*, (Lecture Notes in Physics 837), eds. M.A.L. Marques, N.T. Maitra, F. Nogueira, E.K.U. Gross, and A. Rubio, (Springer-Verlag, Berlin, Heidelberg, 2012).
 [3] PCCP Themed Issue on Time-Dependent Density Functional Theory, Phys. Chem. Chem. Phys. **11**, eds. M. A. L. Marques and A. Rubio (2009).
 [4] J. Autschbach, ChemPhysChem, **10**, 1757 (2009), and references therein.
 [5] T. Stein, L. Kronik, and R. Baer, J. Am. Chem. Soc. **131**, 2818 (2009); R. Baer, E. Livshits, and U. Salzner, Annu. Rev. Phys. Chem. **61**, 85 (2010).
 [6] M. Hellgren and E. K. U. Gross, Phys. Rev. A. **85**, 022514 (2012).
 [7] N. T. Maitra, J. Chem. Phys. **122**, 234104 (2005); N. T. Maitra and D. G. Tempel, *ibid.* **125**, 184111 (2006).
 [8] J. I. Fuks, A. Rubio, and N. T. Maitra, Phys. Rev. A. **83**, 042501 (2011).
 [9] D. G. Tempel, N. T. Maitra, and T. J. Martinez, J. Chem. Theory Comput. **5**, 770 (2009).
 [10] N. Helbig, I. V. Tokatly, A. Rubio, J. Chem. Phys. **131**, 224105 (2009)
 [11] S. Kümmel and L. Kronik, Rev. Mod. Phys. **80**, 3 (2008).
 [12] P. Elliot, J. I. Fuks, N. Maitra and A. Rubio, submitted, arXiv:1211.2012v1 [physics.chem-ph] (2012).
 [13] J. P. Perdew, in *Density Functional Methods in Physics*, edited by R. M. Dreizler and J. da Providencia Plenum, New York, 1985; C. O. Almbladh and U. von Barth, *ibid.*
 [14] O. V. Gritsenko and E. J. Baerends, Phys. Rev. A **54**, 1957 (1996).
 [15] A. Castro *et al.*, Phys. Stat. Sol. (b) **243**, 2465 (2006).
 [16] M. A. L. Marques, A. Castro, G. F. Bertsch, and A. Rubio, Comp. Phys. Comm. **151**, 60 (2003).
 [17] M. Thiele, E. K. U. Gross, and S. Kümmel, Phys. Rev. Lett. **100**, 153004 (2008).
 [18] P. Elliott and N. T. Maitra, Phys. Rev. A. **85**, 052510 (2012).
 [19] N.T. Maitra, K. Burke, and C. Woodward, Phys. Rev. Lett. **89**, 023002 (2002).
 [20] J. I. Fuks, P. Elliott, N.T. Maitra, and A. Rubio, in preparation.
 [21] J. I. Fuks, N. Helbig, I. V. Tokatly, and A. Rubio, Phys. Rev. B. **84**, 075107 (2011).
 [22] A. Brown, W.J. Meath, P. Tran, Phys Rev. A, **63**, 013403 (2000).
 [23] Some degree of spatial and time non-locality is introduced in orbital functionals, such as hybrid functionals that mix in a fraction of non-local exchange [11].
 [24] The Rabi frequency is given within rotating wave approximation by $\Omega_R = \frac{2d_{ge}A}{z} J_1[z]$, where $J_1[z]$ is a Bessel function with argument $z = \frac{(d_{ee}-d_{gg})A}{\omega}$, A and ω are the parameters of the external field and d_{ge}, d_{gg}, d_{ee} are matrix elements that characterize the system (see Ref. [22] for details). The charge-transfer state for our closed-shell fragments model is reached at $T_R/2 = \frac{\pi}{\Omega_R}$
 [25] For smaller separations the approximations perform better, as their character becomes more local; the approximated dipoles are closer to the exact ones, but errors will remain without the non-adiabatic dependence in the potential [12].